Vortex Shear Modulus and Lattice Melting in Twin Boundary Channels of $YBa_2Cu_3O_{7-\delta}$

W. K. Kwok, J. A. Fendrich, V. M. Vinokur, A. E. Koshelev, and G. W. Crabtree

Materials Science Division and Science and Technology Center for Superconductivity, Argonne National Laboratory, Argonne, Illinois 60439

(Received 27 October 1995)

Melting of the vortex lattice is probed directly by investigating the flow of vortices in channels created by twin boundaries. The angular-dependent resistivity $\rho_{T,H}(\theta)$ has a maximum above the melting temperature T_m and crosses over to a minimum below, corresponding to the onset of a shear modulus which reduces vortex flow in the channels. A peak effect in the critical current below T_m is accompanied by a sharp increase in the twin boundary pinning accommodation angle. We calculate the effective twin boundary pinning energy by relating the accommodation angle to a thermal depinning angle. [S0031-9007(96)00329-8]

PACS numbers: 74.60.Ge

Transport measurements in $YBa_2Cu_3O_{7-\delta}$ have yielded strong evidence of a first order vortex melting transition [1–9] in clean homogeneous $YBa_2Cu_3O_{7-\delta}$ crystals. Recently, magnetization measurements in untwinned $YBa_2Cu_3O_{7-\delta}$ crystals have revealed corroborative evidence for this first order melting—a sharp discontinuity at T_m [10,11] similar to that observed in earlier equilibrium measurements on $Bi_2Sr_2CaCu_2O_8$ single crystals [12,13].

A defining characteristic of the melting-freezing transition is the development of a nonzero shear modulus, which leads to a substantial increase in the pinning produced by a given configuration of pinning sites, inducing a sharp drop in resistivity upon freezing [14]. This sharp drop in resistivity is one of the hallmarks of the vortex freezing transition. If the Lorentz force driving the vortices is strong enough to depin the vortex solid, the finite shear modulus affects the vortex motion in another way: it imposes local structure on the moving vortex system. When the shear yield stress is high enough, the vortices move in *elastic flow*, in which translational periodicity is maintained throughout the moving lattice, thus preserving the lattice structure globally. If the shear yield stress is too low, the lattice structure is maintained only locally, allowing neighboring sections of the lattice to move past each other in *plastic flow* [15].

Transport measurements are sensitive to each of these two types of motion and therefore are capable of probing the development of the shear modulus in the solid state. The recent discovery of a peak effect in the critical current density occurring just below the melting temperature [16] and the report of a washboard frequency [17] associated with a moving lattice below T_m in single crystal $YBa_2Cu_3O_{7-\delta}$ suggest that there is a transition between elastic and plastic states of motion as the shear modulus is weakened prior to melting.

In this Letter we investigate the melting of the vortex lattice as it moves inside channels created by parallel twin boundaries in a cleaved $YBa_2Cu_3O_{7-\delta}$ single crystal. Because the average velocity of the vortices in the channels depends strongly on the spatial extent of the local structure and on the pinning strength of the twin boundary channel walls, transport measurements in this geometry are a sensitive probe of the development of the shear modulus. The effective width of the channel and the strength of the pinning at the walls may be varied by tilting the applied magnetic field relative to the twin boundary planes. The angular dependence of the resistivity clearly shows the onset of a nonzero shear modulus at a temperature T_m, which we identify as the freezing-melting temperature. In addition, we observe changes in the vortex dynamics which are correlated with the peak effect in the critical current just below T_m and are indicative of a transition from plastic to elastic flow.

The crystal was grown by a self-flux method [18] which yielded several platelet-shaped crystals. A crystal with only a single set of ⟨110⟩ twin boundaries (TB) was cleaved such that the twin planes were parallel to the short edge of the crystal as shown in the inset of Fig. 1. The crystal dimensions are 1.07 (l) × 0.45 (w) × 0.02 (t) mm^3.

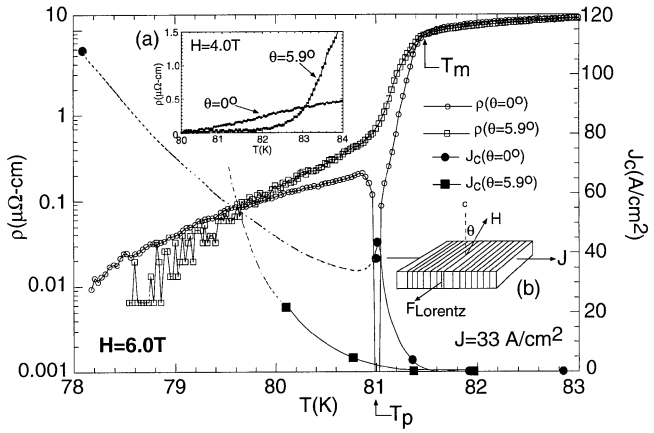

FIG. 1. Resistivity and critical current vs temperature for $H = 6$ T for $\theta = 0°$ ($H \parallel c$) and $\theta = 5.9°$ near the tail of the transition. Inset (a) shows the same for $H = 4$ T below T_m. Inset (b) shows the orientation of the magnetic field, applied current, and twin boundaries.

 0031-9007/96/76(24)/4596(4)$10.00

The average spacing of the twin planes is $d_{\rm ave} = 1.5\ \mu$m and the median spacing is $d_m = 1\ \mu$m. There are approximately 65 twin boundaries between the two voltage contacts. A measuring current perpendicular to the TB and an applied magnetic field along the crystallographic **c** axis induce a Lorentz force on the vortices along the channel direction as shown in the inset to Fig. 1. ac resistivity was measured by the four probe method with current in the **a-b** plane of the crystal and perpendicular to the twin planes. Voltage-current characteristics were measured with a dc current and a nanovoltmeter.

Figure 1 is a logarithmic plot of the *tails* of the temperature dependent resistive transitions in a magnetic field of 6 T oriented parallel to the **c** axis and tilted 5.9° away from the **c** axis. Also shown is the temperature dependence of the critical current at each angle obtained with a 1 μV/cm criterion. We see a sharp drop in the resistivity for both orientations at $T_m = 81.5$ K, associated with the vortex freezing transition [5,6,19]. In earlier studies, such "kinks" in the resistivity curves were observed only in clean untwinned crystals. However, since in this experiment the driving Lorentz force is *parallel* to the twin planes, the flow of the vortices *between* the twin planes is nearly unimpeded by twin boundary pinning. For $H = 6$ T, the vortex spacing is $a_0 \sim 185$ Å. A single channel with a TB spacing of 1 μm thus accommodates about 50 vortices across its width. When the magnetic field is aligned with the **c** axis, these vortices do not intersect either of the bounding twin planes and they are free to move under a Lorentz force parallel to the twin planes. A single twin boundary has an effective width of 10–50 Å [20], which is comparable to the vortex superconducting coherence length $\xi_{ab}(T = 80\ {\rm K}) \sim 44$ Å and provides an ideal single vortex pin site. Thus the number of free vortices within the channels is about an order of magnitude larger than the number of pinned vortices residing on a twin boundary, and the temperature dependence of the resistivity looks very similar to that of untwinned crystals reported earlier [6,19].

Below T_m the resistivity $\rho(\theta = 0°, T, 6\ {\rm T})$ exhibits a sharp drop, reaching a minimum at $T_p = 81.0$ K. This minimum is associated with a sharp maximum ("peak effect") in the critical current $J_c(\theta = 0°, T_p)$. Similar behavior just below the melting temperature in dilutely twinned $YBa_2Cu_3O_{7-\delta}$ crystals was explained by a crossover from plastic to elastic flow, and enhanced pinning arising from the elastic softening of the vortex lattice [16,21]. The softening of the lattice structure allows the vortices to adjust more favorably to a nearby twin boundary pinning site and thus resistivity is decreased [22,23]. The peak effect below the melting temperature T_m is absent at $\theta = 5.9°$ in our experiment, since pinning by the twin boundary sites is reduced in the vortex solid state when the magnetic field is tilted off the twin planes [24]. At lower temperatures the two resistivity curves for $\theta = 0°$ and 5.9° intersect at T = 79.6 K indicating that bulk pinning may overcome twin boundary pinning at lower temperatures [see also inset (a), Fig. 1].

Figure 2 shows our main result, the angular dependence of the resistivity as the magnetic field is tilted symmetrically away from the **c** axis towards the **a-b** plane at $H = 6$ T for a sequence of temperatures. The resistivity at $\theta = 0°$ ($H \parallel c$) shows a dramatic evolution from a maximum above the melting temperature $T_m = 81.50$ K to a minimum below T_m. This pronounced change in behavior is a direct result of the appearance of a nonzero shear modulus at T_m and underlies the use of vortex flow in channels to directly probe the vortex melting transition.

The highest temperature shown, $T = 82.93$ K, is above the onset of twin boundary pinning and there is no feature in $\rho(\theta)$ associated with vortex channel flow. At $T = 82.40$ K, well above the freezing transition, a maximum occurs at $\theta = 0°$ ($H \parallel c$), shown on an expanded scale in Fig. 3(a). This maximum at $\theta = 0°$ is a new feature in the angular dependence of ρ which can be explained by the hydrodynamics in the liquid state and the finite width of the channel. The resistivity falls sharply as the angle from the **c** axis increases from 0 to ±1.8°, then rises again to a broad maximum at $\theta_a = \pm 5°$, after which it decreases monotonically due to the intrinsic anisotropy of the superconducting effective mass.

The behavior of $\rho(\theta)$ can be understood as a geometrical feature related to the finite size of the channels. As the field is tilted from the **c** axis, the number of vortices which intersect the twin boundaries grows, increasing the effective thickness of the channel wall. The number of moving vortices which do not intersect a twin plane is reduced, thus decreasing the effective channel width. This

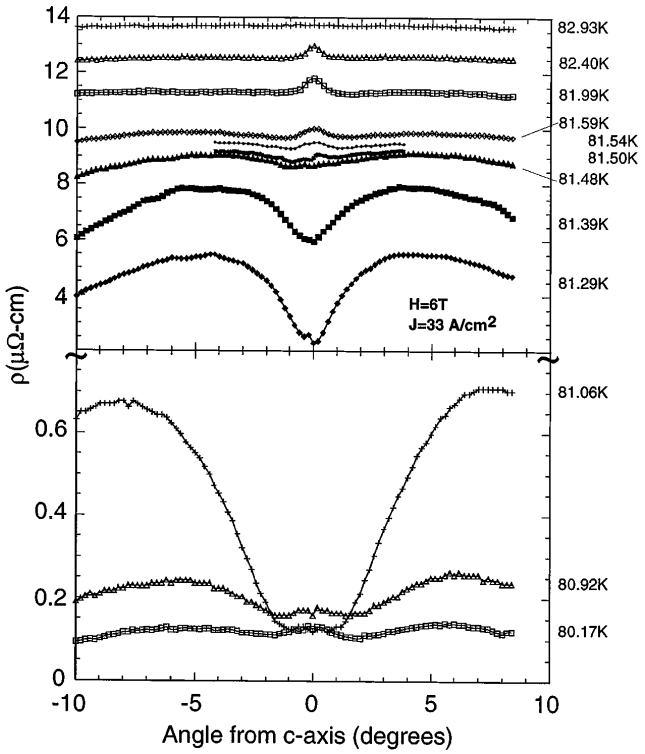

FIG. 2. Angular dependence of the resistivity at $H = 6$ T for $82.93 < T < 80.17$ K.

process continues with increasing angle until, at θ_p, the channel width is effectively zero and all vortices intersect at least one twin plane. An estimate of this angle is provided by $\theta_p = \tan^{-1}(d_m/t) \sim 2.8°$. In practice, the angle will be reduced due to thermal disorder and the elastic nature of the vortices. We believe this reduction of effective channel width explains our observation of the sharp peak in the vortex liquid state resistivity centered at $\theta = 0°$.

For angles greater than θp, the vortices assume a step pattern, the geometry of which is determined by the tilt modulus and the pinning energy [25,26]. The resistivity increases gradually as the angle is increased until, at a large enough angle θ_a, the elastic tilt energy required to maintain the step pattern is too high and the vortices straighten, intersecting the twin boundaries at points. The angle θ_a where the step pattern disappears is marked by a maximum in $\rho(\theta)$, as twin boundary pinning yields to intrinsic anisotropy as the dominant influence on the resistivity. Below we explain the disappearance of the stepped phase at θ_a as a thermal depinning effect.

At lower temperatures, the relative height of the peak at $\theta = 0°$ is reduced with respect to the broad maximum at θ_a, until below the freezing-melting temperature $T_m = 81.50$ K, the peak completely disappears and is replaced by a broad valley which extends in angle to θ_a as illustrated in Fig. 2 [and on an expanded scale in Fig. 3(c)]. The transition from a maximum to a minimum at $\theta = 0°$ indicates a dramatic change in the dynamics of vortex channel flow which occurs over a narrow temperature range of 60 mK. We attribute this change to the formation of a vortex lattice and the *onset of a nonzero vortex shear modulus*. The nonzero shear modulus is associated with the formation of lattice fragments which extends the effective pinning range of the twin boundaries, thereby impeding the flow of vortices in the channels. Therefore the maximum pinning in the vortex solid state is observed when the vortices are aligned with the twin planes.

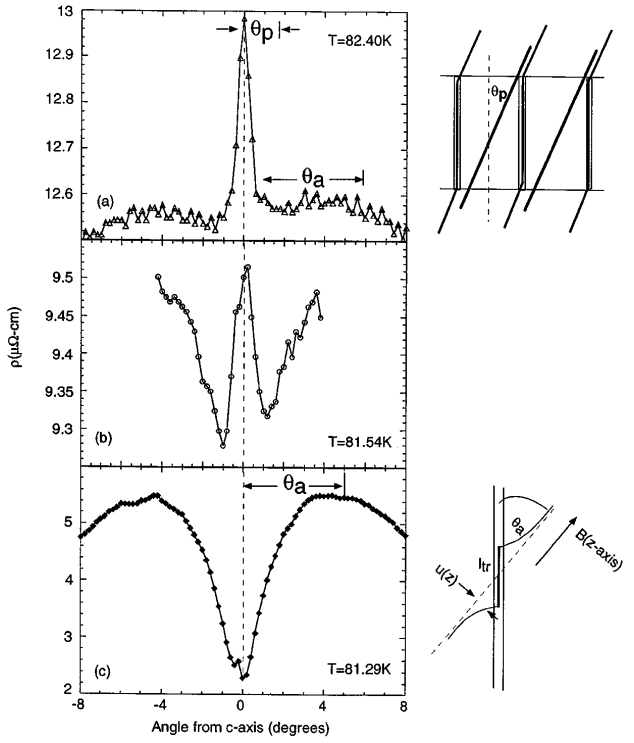

FIG. 3. Enlarged angular dependence of the resistivity at $H = 6$ T for (a) $T = 82.40$ K (vortex liquid state), (b) $T = 81.54$ K (vortex melting-freezing temperature), and (c) $T = 81.29$ K (vortex solid state), with respective vortex-magnetic field–twin boundary geometries.

At T_m [Fig. 3(b)], the angular dependence of the resistivity displays both the narrow peak of width θ_p characteristic of vortex *liquid* channel flow and the broad valley of width θ_a characteristic of vortex *lattice* channel flow. The simultaneous appearance of these features is consistent with the coexistence of liquid and solid phases in a first order phase transition.

Over a 0.5 K range below T_m, the resistivity $\rho(\theta = 0°)$ drops precipitously, reaching a minimum at $T_p = 81.06$ K, below which the resistivity rises again slightly (Fig. 2, lower panel). This temperature dependence is shown in more detail in Fig. 1 for $\theta = 0°$. At T_p the shape of the angular-dependent resistivity is suddenly modified in two respects: The minimum near $\theta \sim 0°$ becomes very broad and the maximum at θ_a jumps from 5° to 8°. The rapid drop in resistivity above T_p indicates that the motion of the vortex solid is severely impeded just below the freezing temperature. We associate this reduced velocity with an increase in the dimensions of the flowing lattice fragments as the solid state becomes established. At T_p, the size of the lattice fragments exceeds the channel width, and the *plastic flow* which characterizes the solid motion just below the melting transition is replaced by *elastic flow*. This is evidenced by the clear maximum in the critical current $J_c(\theta = 0°)$ as the plastic flow process is replaced by elastic flow. The maximum effective pinning is realized at T_p, when the "soft" shear modulus enhances the ability of the vortex lattice to take advantage of the twin boundary pinning sites and settle deeper into their pinning potential wells. The sudden increase in θ_a from 5° to 8° strongly supports the interpretation of the peak effect as an effective increase in the twin boundary pinning strength [23,25].

The shear modulus increases below T_p as temperature is lowered and the lattice becomes more rigid. The enhanced pinning which was observed at T_p because the lattice was "soft" is replaced by less effective pinning as the lattice becomes relatively more rigid, causing the resistivity to increase. The angular dependence of the resistivity also decreases dramatically at lower temperatures as shown by the difference between the $T = 81.06$ and $T = 80.92$ K curves in Fig. 2. One reason may be the enhancement of bulk pinning at lower temperatures. At $T = 79.6$ K, the resistivity curves $\rho(\theta = 0°, T)$ and $\rho(\theta = 5.9°, T)$ intersect, suggesting that bulk pinning becomes more effective than twin boundary pinning at lower temperatures. Recent magneto-optical imaging [27] and magnetization measurements [28] have demonstrated that twin planes are easy paths for flux penetration.

We can calculate the pinning energy of the twin planes from the observed accommodation angle θ_a if we take into account the thermal energies at these temperatures. We identify the experimental accommodation angle $\theta_a \sim 5°$ as the angle at which thermal fluctuations strongly suppress the trapping of the vortex line by twin boundaries. This occurs when $k_B T$ exceeds the pinning energy $E_{\rm pin}(\theta)$ of the trapped vortex segment [see Fig. 3(c)].

The energy of the deformed vortex may be expressed as

$$E = \int dz \left[\frac{\varepsilon_1}{2} \left(\frac{du}{dz} \right)^2 + \frac{K}{2} u^2 \right] - U_p l_{\rm tr} , \qquad (1)$$

where $\varepsilon_1 = [\Phi_0^2/(4\pi\lambda_c)^2] \ln(a_0/\xi)$ is the linear tension of the individual vortex, the term $Ku^2/2$ represents the "cage potential" [29] coming from the interaction with other vortices $K = \Phi_0 B/4\pi\lambda_{ab}^2$, U_p is the pinning potential on the twin boundary, $l_{\rm tr}$ is the length of trapped segment, $E_{\rm pin} = -U_p l_{\rm tr}$, $u(z)$ is the deformation of the line, and the **z** axis is chosen along the magnetic field. The deformed regions of the vortex consist of three segments [26] [see Fig. 3(c)]: the trapped piece with deformation $u(z) = z \tan(\theta)$ at $|z| < l_{\rm tr} \cos(\theta)/2$, and two "healing" regions with deformation $u(z) = l_{\rm tr} \sin(\theta) \exp(-|z - l_{\rm tr} \cos(\theta)/2|/l_{\rm heal})$ at $|z| > l_{\rm tr} \cos(\theta)/2$, where $l_{\rm heal} = \sqrt{\varepsilon_1/K}$ is the "healing length." Substituting these deformations into (1) and minimizing E with respect to $l_{\rm tr}$, we obtain

$$E_{\rm pin}(\theta) = -E_{\rm pin0} \left(1 - \frac{\theta}{\theta_{a0}} \right)^2 \left(\frac{\theta_{a0}}{\theta} + \frac{1}{2} \right), \qquad (2)$$

with the mean-field accommodation angle $\theta_{a0} \approx \sqrt{2U_p/\varepsilon_1}$ [26,27] and the typical pinning energy $E_{\rm pin0} = \frac{4}{3}\sqrt{\varepsilon_1/K}\, U_p$. The angle $\theta_a(T)$ above which trapping by twin boundaries is destroyed by thermal fluctuations can be estimated from the condition $E_{\rm pin}(\theta_a(T)) \sim k_B T$. If $E_{\rm pin0} \ll k_B T$, then the apparent accommodation angle $\theta_a(T)$ is suppressed well below θ_{a0}, and $\theta_a(T) = \theta_{a0} E_{\rm pin0}/k_B T$. We can introduce a dimensionless constant α_p in lieu of $U_p = \alpha_p \varepsilon_0$, where $\varepsilon_0 = \Phi_0^2/(4\pi\lambda_{ab})^2$. The latter expression can then be conveniently rewritten as

$$\theta_a(T) \approx \frac{\alpha_p^{3/2} \varepsilon_0 \sqrt{\Phi_0/B}}{2Tk_B} . \qquad (3)$$

Using the experimentally obtained angle $\theta_a(T) \sim 5°$, we can estimate the effective pinning strength α_p from the latter expression. Taking $B = 6$ T, $T = 81.5$ K, and $\lambda_{ab}(T) = 3000$ Å, we obtain $\alpha_p \sim 0.023$, in good agreement with magneto-optical ($\alpha_p \sim 0.017$) [30] and decoration ($\alpha_p \sim 0.026$) [31] experiments.

In summary, we report direct evidence for the onset of a nonzero shear modulus at the vortex freezing transition in $YBa_2Cu_3O_{7-\delta}$, obtained from the dynamic behavior of vortices in a unique channel flow geometry. We see a new feature in the liquid state, a peak in the angular dependence of the magnetoresistivity for H aligned with the channel walls, which changes suddenly to a valley at T_m due to the appearance of a finite shear modulus in the solid. Below the freezing temperature, we demonstrate new effects on the anisotropy of the magnetoresistivity caused by the premelting peak effect, and show that these effects are consistent with an increase in twin boundary pinning due to a soft shear modulus in the vortex solid. Finally, we show how thermal depinning determines the accommodation angle θ_a and deduce the twin boundary pinning strength, finding good agreement with previous estimates based on vortex decoration and magnetro-optical measurements.

This work was supported by the U.S. Department of Energy, BES Materials Science under Contract No. W-31-109-ENG-38 (W. K. K., V. M. K., G. W. C.) and the NSF Office of Science and Technology Centers under Contract No. DMR91-20000, Science and Technology Center for Superconductivity (J. A. F., A. E. K.).

[1] E. Brezin *et al.*, Phys. Rev. B **31**, 7124 (1985).
[2] D. R. Nelson *et al.*, Phys. Rev. B **39**, 9153 (1989).
[3] E. H. Brandt, Phys. Rev. Lett. **63**, 1106 (1989).
[4] A. Houghton *et al.*, Phys. Rev. B **40**, 6763 (1989).
[5] H. Safar *et al.*, Phys. Rev. Lett. **69**, 824 (1992).
[6] W. K. Kwok *et al.*, Phys. Rev. Lett. **72**, 1092 (1994).
[7] M. Charalambous *et al.*, Phys. Rev. B **45**, 5091 (1992).
[8] J. A. Fendrich *et al.* (to be published).
[9] J. A. Fendrich *et al.*, Phys. Rev. Lett. **74**, 1210 (1995).
[10] R. Liang *et al.*, Phys. Rev. Lett. **76**, 835 (1996).
[11] U. Welp *et al.*, Phys. Rev. Lett. (to be published).
[12] H. Pastoriza *et al.*, Phys. Rev. Lett. **72**, 2951 (1994).
[13] E. Zeldov *et al.*, Nature (London) **375**, 373 (1995).
[14] H. Pastoriza *et al.*, Phys. Rev. Lett. **75**, 3525 (1995).
[15] S. Bhattacharya and M. J. Higgins, Phys. Rev. B **52**, 64 (1995).
[16] W. K. Kwok *et al.*, Phys. Rev. Lett. **73**, 2614 (1994).
[17] J. M. Harris *et al.*, Phys. Rev. Lett. **74**, 3684 (1995).
[18] D. L. Kaiser *et al.*, Appl. Phys. Lett. **51**, 1040 (1987).
[19] W. K. Kwok *et al.*, Phys. Rev. Lett. **69**, 3370 (1992).
[20] G. van Tendeloo *et al.*, Physica (Amsterdam) **167C**, 627 (1990).
[21] For alternate view on T_p and T_m, see X. Ling *et al.* (to be published).
[22] A. B. Pippard *et al.*, Philos. Mag. **19**, 217 (1969).
[23] A. I. Larkin *et al.*, Phys. Rev. Lett. **75**, 2992 (1995).
[24] S. Fleshler *et al.*, Phys. Rev. B **47**, 14 448 (1993).
[25] G. Blatter *et al.*, Phys. Rev. B **43**, 7826 (1991).
[26] E. B. Sonin, Phys. Rev. B **48**, 10 287 (1993).
[27] U. Welp *et al.*, Physica (Amsterdam) **235C–240C**, 241 (1994).
[28] M. Oussena *et al.*, Phys. Rev. B **51**, 1389 (1995).
[29] The effective cage potential describes the nonlocal tilt and compression contributions to the elastic energy in the limit when the typical length scales of deformations are less than λ.
[30] L. A. Dorosinskii *et al.*, Physica (Amsterdam) **246C**, 283 (1995).
[31] L. Y. Vinnikov *et al.*, Superconductivity **3**, 1120 (1990).